MM Science Journal | www.mmscience.eu
ISSN 1803-1269 (Print) | ISSN 1805-0476 (On-line)
Special Issue | VRBA100
International Conference on Modern Manufacturing Technologies
4. 10. 2023, Ostrava, Czech Republic
DOI: 10.17973/MMSJ.2024_02_2023141

VRBA2024-00005

PROPERTIES OF GRADIENT LAYERS OBTAINED THROUGH HVOF SPRAYING AND PLASMA CLADDING

V. Ochodek[1], M. Szymura[2]

[1]VSB – Technical University of Ostrava, Faculty of Mechanical Engineering, Dept. of Mechanical Technology, Ostrava, Czech Republic

[2]Silesian University of Technology, Faculty of Mechanical Engineering, Dept. of Welding, Gliwice, Poland

V. Ochodek, vladislav.ochodek@vsb.cz

Abstract
The study discussed in the article aimed to identify the obtainability of a gradient layer made by the High-Velocity Oxygen Fuel (HVOF)-spraying of an NiAl-based coating between a layer made using the plasma cladding process and powder Stellite 6 and a substrate made of structural steel S355JR. Overlay welds obtained in related tests were made using various process parameters as well as various values of current, travel speeds and powder feed rates. The study also involved the performance of macro and microscopic metallographic tests, hardness measurements as well as the analysis of the chemical and phase composition of gradient layers.

Keywords:
Gradient layer, plasma cladding, Stellite 6, thermal coating, HVOF spraying

1 INTRODUCTION

An important aspect in the engineering design of machinery elements provided with thermally sprayed coatings and deposited layers is the appropriately determined thickness of the surface layer. Thicker coatings and layers characterised by the same resistance to a given wear mechanism undergo tribological wear slower. In addition, thick fault-free coatings are more resistant to corrosive wear. Because of the partial melting of the substrate material during the cladding process, the chemical composition of a newly obtained layer may vary across its thickness [Clyne 1997, Guilemany 2022, Han 2009]. However, an increase in the thickness of the coating and that of the layer is accompanied by an increase in internal stresses, potentially leading to the formation of cracks. The exceeding of the critical value of internal stresses in the deposited coating may lead to its separation from the substrate [Riabcew 2017, Szymura 2021, Tailor 2018]. Obviously, thinner coatings and layers are cheaper to manufacture. Typical thicknesses of HVOF-sprayed coatings are restricted within the range of approximately 100 μm to 300 μm. Typically, the thickness of plasma clad layers exceeds 0,5 mm [Hofman 1998, Ochodek 2018, Pawlowski 2008, Vysoudil 2021].

One of the best-known technological processes enabling the making of gradient layers involves the performance of thermal spraying on a previously deposited layer. Available reference publications do not contain information concerned with the possibility of obtaining a gradient layer by performing the cladding process on a previously deposited coating. The aforesaid lack of information inspired the authors' attempt to obtain a gradient layer through the deposition of a layer on a previously sprayed coating.

The research work-related tests presented below aimed to identify the obtainability of a gradient layer by the HVOF-spraying of a NiAl-based coating between a layer made using the plasma cladding process and powder Stellite 6 and a substrate made of structural steel S355JR. Overlay welds obtained in the tests were made using various process parameters as well as different values of current, travel speeds and powder feed rates. The study also required the performance of macro and microscopic metallographic tests, hardness measurements as well as the analysis of the chemical and phase composition of gradient layers.

2 TEST MATERIALS

The HVOF spraying process involved the use of powder NI-185 (NiAl) (Praxair), the particles of which were obtained through water atomisation. Powder NI-185 is recommended to be used, among other things, as an intermediate coating. The plasma clad layer was obtained using powder CO-106-8 (Stellite 6) (Praxair). According to the manufacturer, layers made using powder CO-106-8 can be exposed to high-temperature-induced wear and corrosive wear conditions. The base material had the form of specimens sampled from a round bar made of steel S355JR and having a diameter of 70,0 mm (in accordance with EN 10025-2). The chemical composition of filler materials is presented in Tab. 1.

Tab. 1: Chemical composition of the filler materials used in the tests.

Filler material	Chemical composition (% by weight)				
	C	Cr	Ni	Mo	W
NI-185	-	-	bal.	-	-
CO-106-8	1,0	28,0	< 2	< 1	4,0
	Fe	Co	Al	Si	Others
NI-185	-	-	5,0	-	-
CO-106-8	< 2	bal.	-	1,0	< 1

3 TEST

3.1 Technological conditions of the cladding process

The tests involved the plasma cladding of single-layer overlay welds (made using powder CO-106-8) on an approximately 0,1 mm thick HVOF-sprayed intermediate coating (made using powder NI-185). The test overlay welds were made using various process parameters, including various values of current, travel speeds and powder feed rates. The technological parameters of the cladding process are presented in Tab. 2.

Tab. 2: Parameters of the cladding process performed using powder CO-106-8.

Specimen designation	Primary arc current, (A)	Travel speed, (cm/min)	Powder feed rate, (g/min)
I	100	3,5	33,2
II	90	4,5	24,9
III	120	4,5	33,2
IV	105	5,0	24,9
Girth cladding in the flat position (PA); plasma gas: 100% Ar, plasma gas flow rate: 3,0 l/min; shielding gas: Ar (bal.) + 2,9% H_2; shielding gas flow rate: 7,0 l/min; weaving move width: 2,0 mm.			

3.2 Macro and microscopic metallographic tests

To identify the quality of the gradient layers it was necessary to perform macro and microscopic metallographic tests using a light microscope and cross-sectional metallographic specimens. The macroscopic metallographic test results are presented in Fig. 1, whereas the microscopic metallographic test results are presented in Fig. 2. The macrostructural photographs were used to calculate (on a computer-aided basis) the geometrical dimensions of the overlay welds. The dilution was determined using the planimetric method and formula (1). The values of dilution in individual specimens are presented in Tab.3.

$$D = \frac{A_{bm}}{A_{bm} + A_r} \cdot 100\ \% \quad (1)$$

where
D – dilution, %;
A_{bm} – area of base metal melted, mm^2;
A_r – area of reinforcement of the deposit, mm.

Tab. 3: Dilution.

Specimen designation	Dilution, (%)
I	19,6
II	46,5
III	38,2

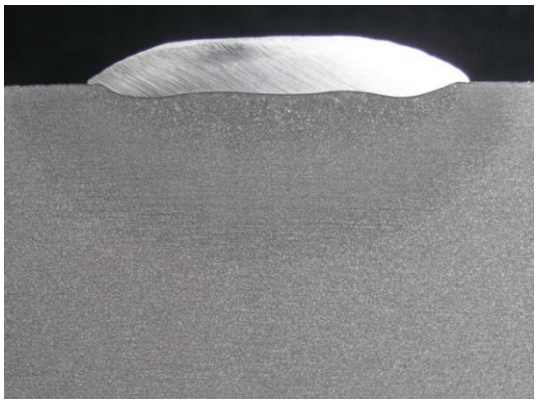

a)

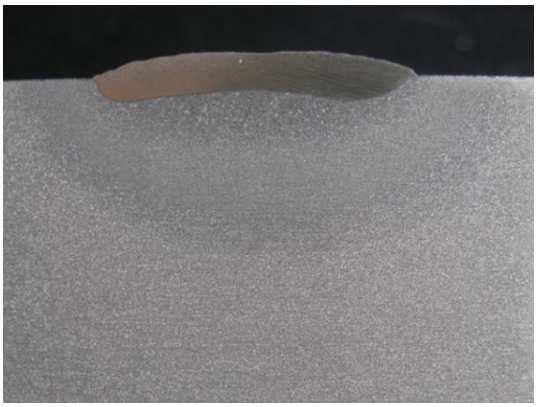

b)

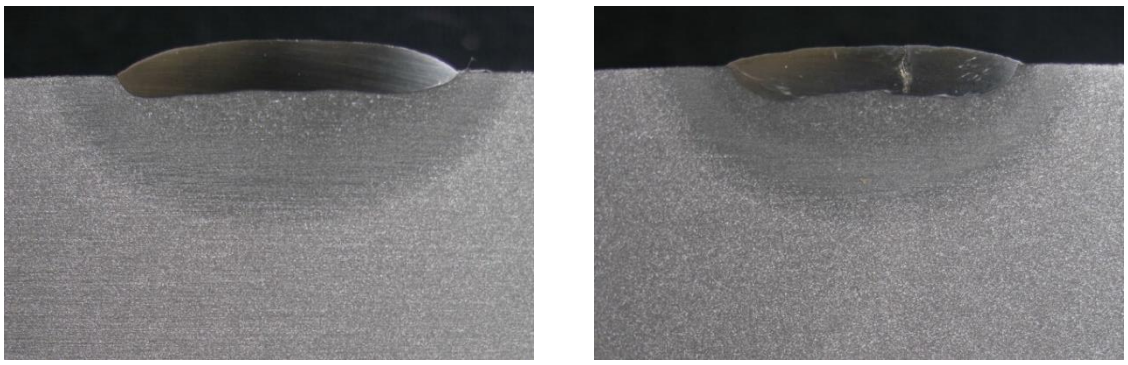

c) d)

Fig. 1. Macrostructure of the gradient layers made using powder CO-106-8 in relation to various values of primary arc current, travel speeds and powder feed rate (Table 2); designation of layers: a) I; b) II; c) III and d) IV; mag. 3,5x.

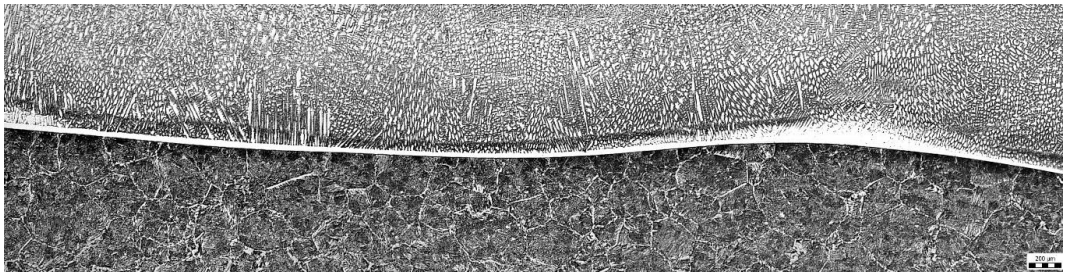

a)

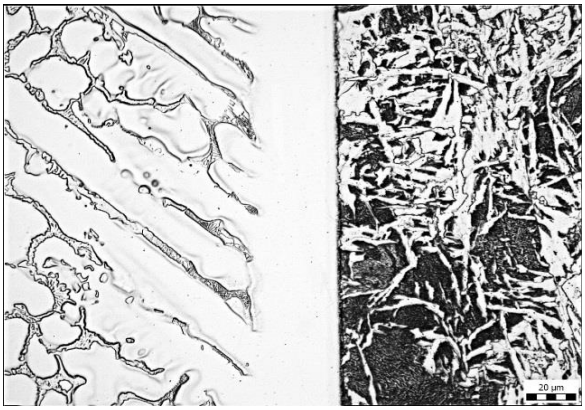

b)

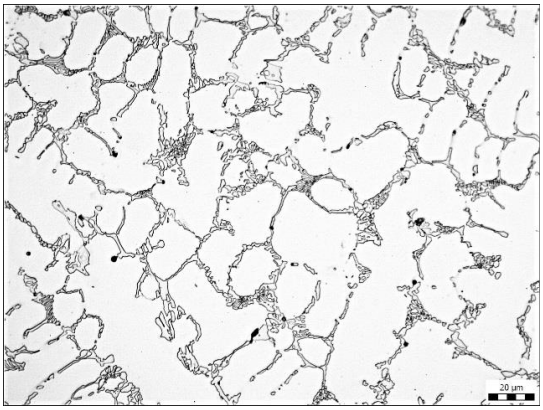

c)

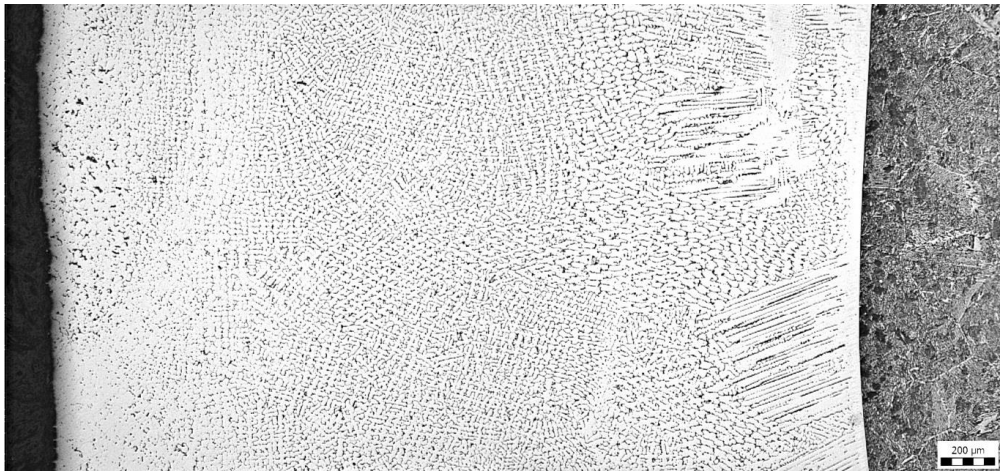

d)

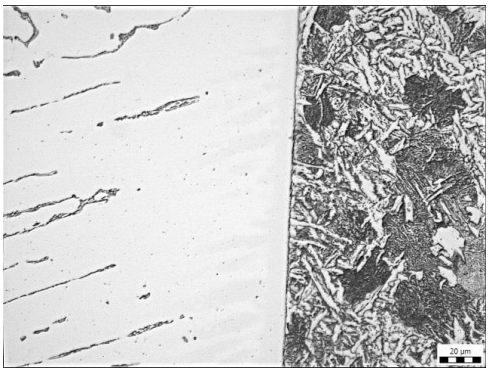

e)

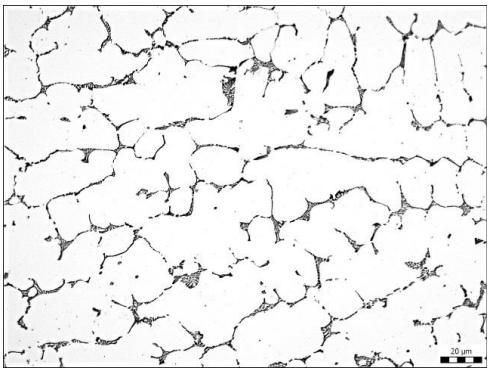

f)

Fig. 2: Microstructure of the gradient layers made using powder CO-106-8: a) HVOF-sprayed NiAl coating of the gradient layer of specimen I; b) HVOF-sprayed NiAl coating of the gradient layer of specimen I; c) overlay weld of specimen I; d) gradient layer of specimen III across its entire height; e) HVOF-sprayed NiAl coating of the gradient layer of specimen III and f) overlay weld of specimen III.

3.3 Hardness measurements

The hardness of the gradient layers made using the plasma cladding process and powder CO-106-8 was identified using the Vickers hardness test and a load of 49,03 N (in accordance with the EN ISO 6507-1standard). The measurements involved the cross-section of the gradient layer, the heat affected zone (HAZ) and the base material. Analogous measurements of microhardness involved specimens designated as I and III. The hardness test results are presented in Fig. 3 and 4.

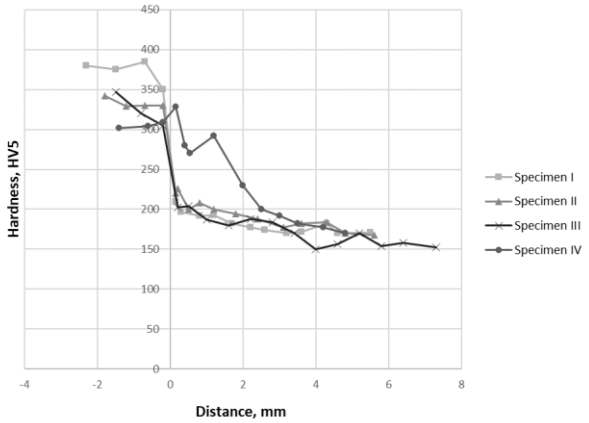

Fig. 3: Results of hardness measurements (HV5) of the gradient layer, heat affected zone and of the base material on the cross-section of the plasma clad specimens made using powder CO-106-8 on the previously HVOF-sprayed NiAl coating.

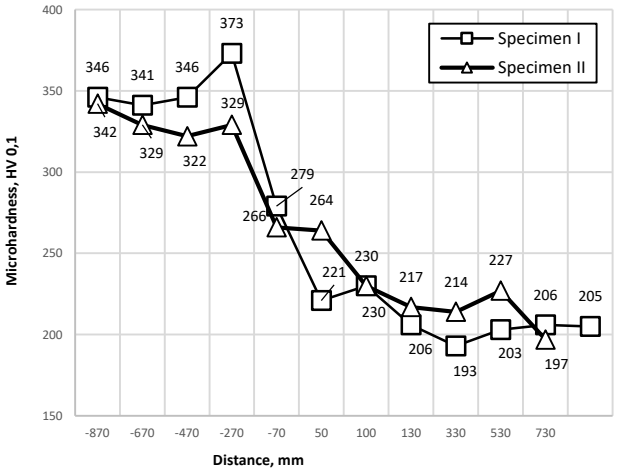

Fig. 4: Results of microhardness measurements (HV0.1) of the gradient layer, heat affected zone and of the base material on the surface of the cross-section of the plasma clad specimens made using powder CO-106-8 on the previously HVOF-sprayed NiAl coating.

3.4 Chemical composition analysis

The chemical composition of specimens I and III was analysed using a scanning electron microscope (SEM). The measurements involved the micro-areas of the deposited layer, the HVOF-sprayed NiAl coating and the substrate material. The chemical composition analysis results are presented in Fig. 5.

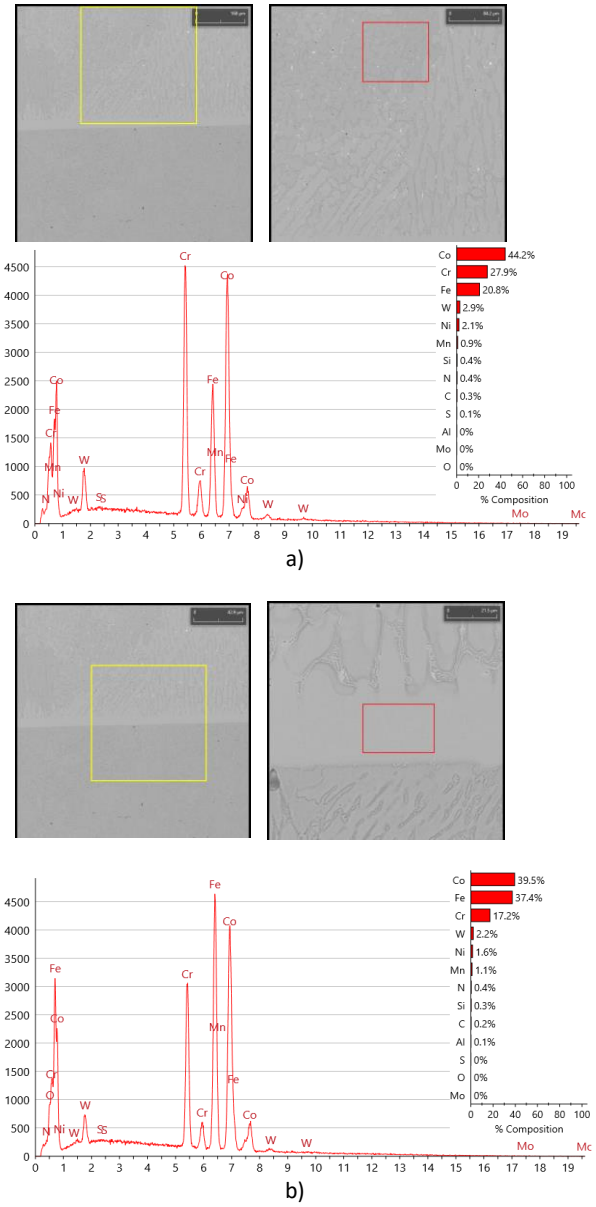

Fig. 5: Micro-area with the results of the SEM-based chemical composition analysis: a) deposited layer (specimen I) and b) HVOF-sprayed NiAl coating (specimen I).

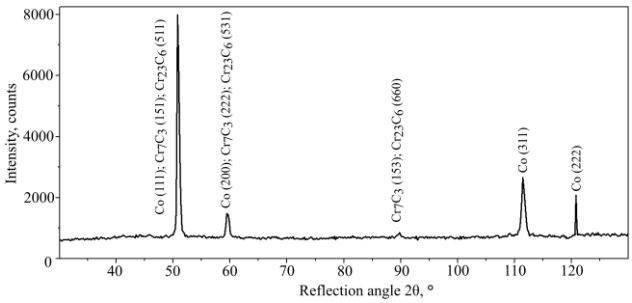

Fig. 6: XRD pattern of the single-layer single-run overlay weld made using the plasma cladding process and powder CO-106-8 (specimen I).

4 CONCLUSIONS

The above-presented tests revealed the obtainability of a gradient layer through the plasma-based deposition of a layer (performed using powder CO-106-8 (Stellite 6)) on a previously HVOF-sprayed NI-185 coating (NiAl). The gradient layers obtained in the tests were characterised by variable properties, which could be of key importance in certain industrial applications (e.g. in relation to surface layers of balls in ball bearings used in the chemical industry).

The metallographic tests did not reveal the presence of welding imperfections in the specimens of gradient layers designated as I, II and III. The specimen of overlay weld IV, made using a primary arc current of 105 A, a travel speed of 5,0 cm/min and a powder feed rate of 24,9 g/min, contained a crack. In accordance with the EN ISO 15614-7 standard, cracks are unacceptable in layers intended for operation in a corrosion environment.

The values identified in the hardness measurements involving the cross-sections of the gradient layers were restricted within the range of 302 HV5 to 380 HV5. The average hardness values concerning individual specimens were restricted within the range of 305,0 HV5 to 372,5 HV5; the largest range amounting to 42 HV5. The highest average hardness was that of specimen I (characterised by the lowest dilution), whereas the lowest average hardness was identified in specimen IV (characterised by the highest dilution). In terms of specimen I, the hardness of the heat affected zone and that of the base material was restricted within the range of 170 HV5 to 210 HV5. In terms of specimen II, the hardness of the heat affected zone and that of the base material was restricted within the range of 168 HV5 to 226 HV5. In terms of specimen III, the hardness of the heat affected zone and that of the base material was restricted within the range of 150 HV5 to 204 HV5, whereas in terms of specimen IV, the hardness of the heat affected zone and that of the base material was restricted within the range of 170 HV5 to 328 HV5. In all of the above-presented cases, hardness values did not exceed the maximum acceptable hardness value of 380 HV5 (in accordance with the EN ISO 15614-7 standard, in relation to steels from material group 1 not subjected to heat treatment). The microhardness of specimen I measured in the cross-section of the gradient layer was restricted within the range of 279 HV0,1 to 373 HV0,1, whereas the microhardness of specimen III measured in the cross-section of the gradient layer was restricted within the range of 266 HV0,1 to 342 HV0,1. The gradient layers were characterised by varied microhardness, increasing from the fusion zone and the sprayed intermediate coating up to the clad layer.

The analysis of the chemical and phase composition as well as the results of the microscopic metallographic tests revealed that, in all variants, the structure of the overlay weld contained the cobalt-based matrix and precipitates of eutectic carbides (Cr_7C_3 and $Cr_{23}C_6$). The chemical composition analysis revealed that the content of Co and that of Cr decreased along with a decreasing distance to the fusion area in the layer. In terms of specimen I, the content of Co decreased from 44,2% to 39,5%, whereas the content of Cr decreased from 27,9% to 17,2%. In turn, as regards specimen III, the content of Co decreased from 34,7% to 29,2%, whereas the content of Cr decreased from 17,9% to 14,6%. The above-presented varying contents resulted from varying dilution; dilution in specimen I amounted to 19,6%, whereas that in specimen III amounted to 38,2%.

The above-presented tests could constitute the basis for the extension of the application potential of the technology discussed in the article.

5 ACKNOWLEDGMENTS

The results of the contribution were achieved by solving the specific research project No. SP2023/020 with the name ”Research and Optimisation of Engineering Technologies” solved in 2023 at the Faculty of Mechanical Engineering of VSB – Technical University of Ostrava**.**

6 REFERENCES

[Clyne 1997] Clyne T. W. et al. Residual stresses in thermal spray coatings and their effect on interfacial adhesion: a review of recent work. Journal of Thermal Spray Technology, 1996, Vol. 5, No.4, pp. 401-418. ISSN 1059-9630.

[Guilemany 2022] Guilemany J. M. et. al. Effects of thickness coating on the electrochemical behaviour of thermal spray Cr3C2–NiCr coatings. Surface and coatings technology, 2022, Vol. 153, No. 2-3, pp. 107-113. ISSN: 0257-8972.

[Han 2009] Han M.S. et. al. Effects of thickness of Al thermal spray coating for STS 304. Transactions of Nonferrous Metals Society of China, 2009, Vol. 19, pp. 925-929. ISSN 1003-6326.

[Hofman 1998] Hofman R. et. al. Electrochemical methods for characterisation of thermal spray corrosion resistant stainless steel coatings. Materials Science Forum, 1998, Vol. 289, pp. 641-654. ISSN 1662-9752.

[Ochodek 2018] Ochodek, Vl. et. al. Evaluation selected characteristic of HVOF coatings In: Proceedings of the 22th International Conference on Metallurgy and Materials (Metal 2018), Ostrava: Tanger, 2018, pp. 1194-1197. ISBN 978-808729484-0.

[Pawlowski 2008] Pawlowski L. The science and engineering of thermal spray coatings. John Wiley & Sons Ltd, 2008, Chichester, pp. 89. ISBN:9780471490494.

[Riabcew 2017] Riabcew I. A. et. al. Welding Imperfections in Surfaced Layers. Biuletyn Instytutu Spawalnictwa, 2017, vol. 3, pp. 26-35. PL ISSN 0867-583X.

[Szymura 2021] Szymura M. Effect of the angle of incidence of abrasive particles on the erosive wear resistance of HVOF-sprayed composite coatings. The Paton Welding Journal, 2021, vol. 10, pp. 47-51. ISSN 0957-798X.

[Tailor 2018] Tailor S. et. al. High-performance molybdenum coating by wire–HVOF thermal spray process. Journal of Thermal Spray Technology, 2018, vol. 27, no. 4, pp. 757-768. ISSN 1059-9630.

[Vysoudil 2021] Vysoudil, F. et. al. Thermal coatings properties by duplex technology. In: Proceedings of the 30th Anniversary International Conference on Metallurgy and Materials (Metal 2021), Ostrava: Tanger, 2021, pp. 446–470. ISBN 978-808729499-4.

CONTACTS:

Ing. Vladislav Ochodek, Ph.D.
VSB – Technical University of Ostrava, Faculty of Mechanical Engineering, Dept. of Mechanical Technology
17. listopadu 2172/15, Ostrava-Poruba, 708 33, Czech Republic
+420597323513, vladislav.ochodek@vsb.cz, www.fs.vsb.cz

Dr.MSc. Michal Szymura
Faculty of Mechanical Engineering, Silesian University of Technology, Faculty of Mechanical Engineering, Welding Department, Konarskiego 18A, 44-100 Gliwice, Poland